THE ASTROPHYSICAL JOURNAL, 429:325–330, 1994 July 1

POLAR CAP MODELS OF GAMMA-RAY PULSARS: EMISSION FROM SINGLE POLES OF NEARLY ALIGNED ROTATORS

JOSEPH K. DAUGHERTY
Computer Science Department, University of North Carolina at Asheville, NC 28804
AND
ALICE K. HARDING
Laboratory for High Energy Astrophysics, NASA/Goddard Space Flight Center, Greenbelt, MD 20771
Received 1993 November 4; accepted 1994 January 4

ABSTRACT

We compare a new Monte Carlo simulation of polar cap models for gamma-ray pulsars with observations of sources detected above 10 MeV by the *Compton Observatory*. We find that for models in which the inclination of the magnetic axis is comparable to the angular radius of the polar cap, the radiation from a single cap may exhibit a pulse with either a single broad peak as in PSR 1706−44 and PSR 1055−52, or a doubly peaked profile comparable to those observed from the Crab, Vela, and Geminga pulsars. In general, double pulses are seen by observers whose line of sight penetrates into the cap interior and are due to enhanced emission near the rim. For cascades induced by curvature radiation, increased rim emission occurs even when electrons are accelerated over the entire cap, since electrons from the interior escape along magnetic field lines with less curvature and hence emit less radiation. However, we obtain better fits to the duty cycles of observed profiles if we make the empirical assumption that acceleration occurs only near the rim. In either case, the model energy spectra are consistent with most of the observed sources. The beaming factors expected from nearly aligned rotators, based on standard estimates for the cap radius, imply that their luminosities need not be as large as in the case of orthogonal rotators. However, small beam angles are also a difficulty with this model because they imply low detection probabilities. In either case the polar cap radius is a critical factor, and in this context we point out that plasma loading of the field lines should make the caps larger than the usual estimates based on pure dipole fields.

Subject headings: gamma rays: theory — pulsars: general — radiation mechanisms: nonthermal

1. INTRODUCTION

Prior to the launch of the *Compton Gamma Ray Observatory* (*CGRO*) in 1991 April, the only confirmed gamma-ray pulsars were the Crab and Vela (PSR 0531+21, PSR 0833−45). To date *CGRO* has made detailed observations of these objects (Nolan et al. 1993; Kanbach et al. 1994) and added four new sources to the list. These include the radio pulsars PSR 1509−58 (Wilson et al. 1992), PSR 1706−44 (Thompson et al. 1992), and PSR 1055−52 (Fierro et al. 1993). The Geminga object, long known to be an intense gamma source (Kniffen et al. 1975; Bennett et al. 1977), has also been found to be a pulsar at both X-ray and gamma-ray energies (Halpern & Holt 1992; Bertsch et al. 1992; Mayer-Hasselwander et al. 1993). The enlarged database of known sources has brought the usual list of new puzzles as well as insights. Each object has at least one distinguishing property that causes problems for classification schemes. For example, all the sources but PSR 1509−58 have detectable emission above 100 MeV, and all are radio pulsars except for Geminga. Only the Crab has gamma-ray pulses in phase with pulsed emission at all other wavelengths, from radio to hard X-rays.

There are also some striking features which several of these sources have in common, especially at the high energies covered by the Compton Telescope (COMPTEL) and the Energetic Gamma Ray Experiment Telescope (EGRET) on board the *CGRO*. Three objects, namely, the Crab (Nolan et al. 1993), Vela (Hermsen et al. 1992; Kanbach et al. 1994), and Geminga (Mayer-Hasselwander et al. 1994), have doubly peaked pulse profiles at energies above 10 MeV. While the relative photon counts and duty cycles of the two peaks are energy dependent, they tend to be comparable in the range 10 MeV–1 GeV. In EGRET data the Crab has the greatest asymmetry between the first and second peaks, with a count ratio ~ 0.2, but comparisons with earlier *SAS-2* and *COS-B* observations suggest a possible secular variation (Kanbach 1990; Nolan et al. 1993). A low-intensity interpulse structure has been seen in all the doubly peaked sources, although it is perhaps significant that no object appears to have more than two "main" peaks. The separation in phase between the peaks is about 0.4 for the Crab and Vela and 0.5 for Geminga. While not statistically significant, the similarity in these values is interesting.

The two objects which appear to have a singly peaked structure (PSR 1706−44, PSR 1055−52) both have comparatively large duty cycles. Unfortunately, the observations to date do not reveal much detail in the pulse profiles.

The spectra of all the sources detected above 100 MeV can be reasonably fitted to power laws whose photon spectral indices γ lie in the range 1.2–2.3. This common power-law dependence is in contrast to the situation at lower energies, where breaks or rollovers are observed over a wide range of energies. At least in the case of Geminga, there is also clear evidence for a spectral steepening or cutoff above a few GeV (Mayer-Hasselwander et al. 1994).

In this work, we attempt to interpret some of these recent observations in terms of the polar cap model of gamma-ray emission (Sturrock 1971; Ruderman & Sutherland 1975; Harding 1981; Daugherty & Harding 1982). For this purpose

we have developed a new Monte Carlo simulation of cascade showers in pulsar magnetospheres, which incorporates significant improvements over an earlier calculation of this type (Daugherty & Harding 1982). In the following, we describe the improvements in the new simulation and discuss its use in empirical investigations of polar cap models. In particular, we show that models in which the magnetic and rotational axes are nearly aligned, and in which the primary electron beam is concentrated around the rim of the polar cap, can reproduce basic features of the observed pulse profiles and energy spectra.

2. SIMULATION OF PAIR CASCADES

Our simulations are based on the traditional features of polar cap models. The key assumption in these models is that electrons (or positrons) are accelerated to very high energies, approaching 10 TeV (Ruderman & Sutherland 1975; Arons 1983), just above the neutron star surface. In the standard model this acceleration is electrostatic in origin and is thought to occur only along the "open" magnetic field lines extending outward from the neutron star to the velocity-of-light cylinder. We assume that the height of the acceleration region is small compared to the polar cap radius. Our simulation traces each primary electron from the height at which it has achieved a maximum "injection" energy.

We assume that the magnetic field lines above the polar caps are purely dipolar. For nearly aligned rotators, the caps should be almost circular with a radius $\rho_{pc} = a\theta_{pc}$, where a is the radius of the neutron star and the angle θ_{pc} is usually estimated from

$$\sin \theta_{pc} = \left(\frac{a}{r_{lc}}\right)^{1/2} = \left(\frac{a\Omega}{c}\right)^{1/2} \quad (1)$$

where $r_{lc} = c/\Omega$ denotes the distance to the light cylinder and Ω is the pulsar rotation frequency. Equation (1) assumes that a pure dipole field line, emerging from a point near the rim of the polar cap, should close just inside the light cylinder. However, since this estimate ignores distortion of the magnetic field by the ambient plasma, it should really be regarded only as a lower limit on θ_{pc}. In fact, simple models assuming a force-free, rigidly corotating plasma (without inertial effects or outward current flow) show a cusplike distortion of the field lines which would effectively increase the polar cap radius by a factor ~ 1.3 (see, for example, Michel 1982, 1991).

As each primary electron coasts outward along its local field line, it loses energy due to curvature radiation (CR). At this stage, a recursive algorithm follows each photon from its creation point, until it either escapes the magnetosphere or is pair-converted by the intense magnetic field. We use attenuation coefficients which cover both near-threshold conversion (Daugherty & Harding 1983; Baring 1988) as well as the high-energy, low-field asymptotic limit (Erber 1966).

If pair conversion occurs, each member of the created pair emits a rapid burst of synchrotron radiation (SR). The SR emission rate is in fact so fast [$\sim 10^{15}(B/B_{cr})^2$ s^{-1}] that we consider the entire burst or SR photons to be emitted at the pair-creation point. We sample the quantized SR emission spectrum using transition rate tables developed by Harding & Preece (1987), which allow us to follow the burst down into the low-energy cyclotron radiation regime. Each SR photon is itself traced by the recursive algorithm, until all the photons which escape have been tallied in three-dimensional tables according to their energies and emission angles. Our method permits us to track the development of cascades through arbitrary generations.

This complete process is carried out for a large ensemble of primary electrons distributed over a polar cap. In the work reported here we have considered two simple primary beam patterns, namely, a uniform distribution over the entire polar cap, and also a hollow cone pattern in which primaries are emitted uniformly around the rim.

3. PULSE PROFILES FROM A SINGLE POLAR CAP

Until quite recently most workers assumed that polar cap models could only account for the doubly peaked pulse profiles seen in the Crab, Vela, and Geminga by requiring these objects to be nearly orthogonal rotators (Harding & Daugherty 1992). In this picture the two peaks correspond to emission seen from opposite magnetic poles. Of course only observers situated near the equatorial plane of the pulsar could detect the two pulses. Given the small beam widths expected from the conventional estimate (1) for the polar cap radius, this is a stringent requirement. The fact that three of the sources discovered to date have double pulses would imply that many if not most of these objects are almost perfectly othogonal rotators.

Another well-known problem with this picture is the ~ 0.4 phase separation between the two peaks in the Crab and Vela pulsars. Even if the inclination of the magnetic axis is not quite $\pi/2$, a dipole field whose axis passes through the center of the neutron star must produce pulses with very nearly 0.5 phase separation in the polar cap model. Thus the orthogonal rotator scenario seems to require additional, ad hoc assumptions such as an off-axis dipole geometry.

In a recent work on cascades initiated by inverse-Comptonized gamma emission from polar caps, Sturner & Dermer (1994) have pointed out that double pulses with large interpulse separations can be observed from a single magnetic pole if the rotation and magnetic axes are nearly aligned. We have independently noted this same effect in our own simulations of CR-induced cascades, and in this section we analyze the geometrical properties required for single polar caps to produce double pulses resembling the observed profiles. In § 4 we consider statistical aspects of the model, including probabilities for detection of the beam and the distribution of peak-to-peak phase separations in double pulse profiles.

Figure 1 depicts the emission cone from a single magnetic polar cap, for a dipole field whose axis is inclined at an angle α with respect to the rotation axis Ω. Since we consider nearly aligned rotators ($\alpha \ll 1$), we may assume a circular cap boundary with angular radius θ_{pc} (not shown). If gamma emission is produced just above the cap surface along directions tangent to the local dipole field lines, the half-angle of the conical emission beam is just $\theta_b = 3\theta_{pc}/2$. Note that the circle drawn around the magnetic pole in Figure 1 has angular radius θ_b, so that it depicts the angular extent of the emission beam rather than the polar cap radius.

Consider an observer O situated at a polar angle ζ, measured with respect to the rotational axis. As shown in Figure 1, the line of sight to O will intersect the edges of the rotating conical beam at azimuthal angles $\pm\phi$ if $|\cos \phi| < 1$, where

$$\cos \phi = \frac{\cos \theta_b - \cos \alpha \cos \zeta}{\sin \alpha \sin \zeta} . \quad (2)$$

If the radiation were emitted uniformly over the entire polar cap, the azimuthal width of the observed pulse would be given

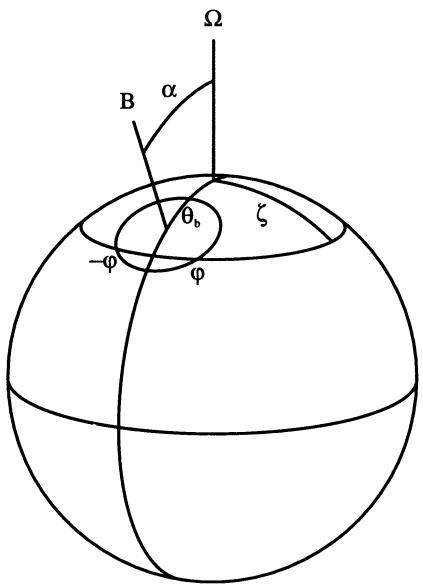

FIG. 1.—Schematic of neutron star polar cap geometry. Inclination of magnetic axis is denoted by α and is assumed small (nearly aligned rotator). Polar cap is nearly circular with angular radius θ_{pc} (not shown). Observer at angle ζ sees edges of conical radiation beam, with half-angle $\theta_b = 3\theta_{pc}/2$, at intersection points labeled by azimuthal angles $\pm\phi$.

by $\delta\phi = 2\phi$. For hollow cone emission, however, $\delta\phi/(2\pi)$ actually represents the phase separation between two distinct peaks, corresponding to the leading and trailing intersection points of the emission cone with the locus of observer positions ζ = constant. For nearly aligned rotators, or more precisely whenever $\zeta \sim \alpha \lesssim \theta_b$, it is possible to obtain values of $\delta\phi \sim \pi$ corresponding to phase separations near 0.5.

It turns out that a hollow-cone emission pattern is expected from any polar cap cascade induced by curvature radiation, even if the primary electron current is essentially uniform over the polar cap surface. This is just due to the fact that the curvature of the field lines tends to vanish in the vicinity of the dipole axis. As Figure 2*a* shows, nearly aligned rotators with uniform primary beams can be seen by observers with $\zeta \sim \alpha$ to emit well-defined double pulses from cascades above a single magnetic pole. However, the duty cycles of the model profiles tend to be larger than those seen from the sources observed to date.

If the primary electron beam itself is concentrated along the outer rim of the polar cap, the emission from a single polar cap can produce double pulses with duty cycles resembling those of the Crab, Vela, and Geminga pulsars. Examples for the Crab are shown in Figures 2*b* and 2*c*. These plots were generated by an ensemble of primary electrons distributed uniformly along the rim. The gamma beam pattern can be understood in terms of the cone generated by the tangents to the local magnetic field at points on the rim. As shown in Figure 2*b*, the escaping cascade radiation includes essentially no emission from the interior of the tangent cone. However, significant emission is produced over extended regions exterior to the cone. Depending on which peak is plotted first in the pulse profile (see § 4), this emission may appear between the first and second peaks, as shown, for example, in Figure 2*c*. In this case, the emission exterior to the main conical beam might account for the weaker interpulse structure observed between the two peaks.

The intense core of cascade photons, concentrated around

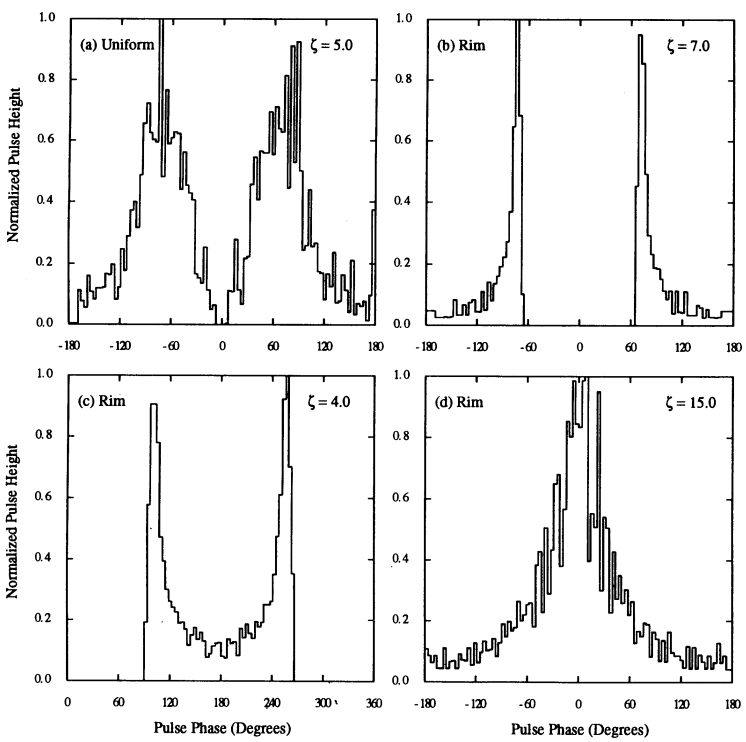

FIG. 2.—Sample pulse profiles for photons above 100 MeV, assuming parameters in Table 1, period of Crab pulsar, and $\alpha = 5°$. Phase angle is identical to angle ϕ in Fig. 1, so that $\phi = 0°$ occurs when observer lies in plane of meridian through polar cap center. (*a*) Profile for cascade initiated by primary beam distributed uniformly over entire polar cap, for observer angle $\zeta = 5°$. (*b*) Profile for primary beam distributed uniformly around polar cap rim (no interior component), for $\zeta = 7°$. (*c*) Profile for rim beam as in (*b*), for $\zeta = 4°$. Range of phase angle is offset by 180°, so that peak-to-peak phase separation appears similar to (*b*). Emission from region outside main conical beam now appears between peaks. (*d*) Rim beam, for $\zeta = 15°$. In this case observer always lies outside main emission cone and sees only a single broad pulse.

the rim, has a softer spectrum than the pure CR emission produced by primary electrons higher above the stellar surface. This is consistent with observations in that the interpulses tend to exhibit harder spectra than the peaks.

We also note that observers whose viewing angles ζ place them near but always outside the cone may see only a single broad peak, as for example in Figure 2*d*. This sort of profile appears similar to those of PSR 1706−44 and PSR 1055−52.

4. STATISTICAL PROPERTIES OF SINGLE-POLE MODELS

Solutions for the quantity $\delta_p = \delta\phi/2\pi$, giving the phase separation between the peaks, can range between 0 and 1. However, observers might choose to define the "first" peak in a double-pulse profile in such a way that the separation never exceeds 0.5. In this case the separation would be given by $\delta_{p2} = \min(\delta_p, 1 - \delta_p)$. We will assume this convention in the following analysis.

It is useful to consider δ_{p2} as a function of the inclination α and observer angle ζ, treating the beam angle θ_b as a parameter. Contour plots of δ_{p2} versus cos (α) and cos (ζ) are shown in Figure 3, for several values of θ_b. The innermost contour in each plot encloses the region in which δ_{p2} ranges between 0.4 to 0.5. Each gamma-ray pulsar observed from the Earth may be represented as a point within a plot of this type. Since we expect the observer to be randomly oriented with respect to the rotation axis Ω, these points should be uniformly distributed along the vertical, or cos (ζ), axis. On the other hand, the distribution of values for cos (α) is unknown. If it should prove to be a nonuniform distribution biased toward small values of α (nearly aligned rotators), most pulsars would be represented by points near the right side of these diagrams.

These plots reveal some general properties of models based on nearly aligned rotators. In particular, they provide information on the fraction of these objects which might be observable from the Earth. The standard estimate (1) for the cap size predicts beam angles θ_b well below 10° for all the gamma-ray pulsars observed to date. However, Figure 3*a* shows that less than 1% of all pulsars with such narrow beams should be oriented toward Earth in such a way as to exhibit double pulses from a single pole with phase separations above 0.4, even if all pulsars had favorable (small) values of α. An even smaller fraction of pulsars should be observable if α has a broad distribution of values. (Of course we should recall that for these same beaming factors, even orthogonal rotators would have detection probabilities ~0.1 or less.) On the other hand, we note from Figure 3*b* that the single-pole model becomes more credible in terms of observability as θ_b is increased.

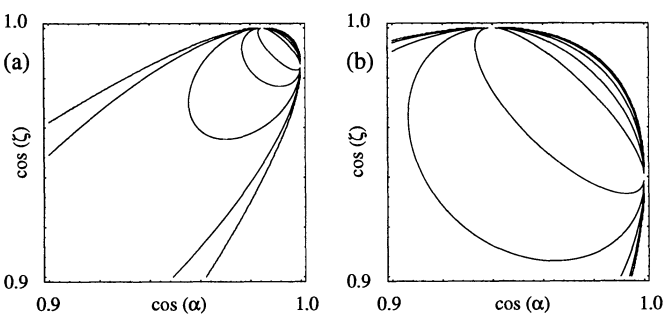

FIG. 3.—Contour plots of phase separation δ_{p2} as function of inclination α and observer angle ζ, treating conical beam half-angle θ_b as parameter. Plots use cosines of α, ζ since random observer directions imply uniform distribution for cos (ζ). Contours divide range 0–0.5 into 5 equal increments, with innermost contour enclosing points for which $0.4 < \delta_{p2} < 0.5$. (*a*) $\theta_b = 10°$; (*b*) $\theta_b = 20°$.

A second point is that even for values of α which make phase separations greater than 0.4 possible, the uniform distribution in cos (ζ) generally makes it more probable to observe smaller separations. The present sample of five sources observed at energies over 10 MeV contains three objects with separations above 0.4. The single-pole model predicts that as the statistics improve, the majority of sources should display either doubly peaked pulse profiles with separations below 0.4 (which for low values may be indistinguishable from single pulses) or single pulses due to emission just outside the polar cap rim. In the latter case, the emission should have a harder spectrum since it is composed primarily of CR photons generated outside the cascade region.

5. ENERGY SPECTRA

Figure 4 shows our model photon spectra for the same primary electron distributions, inclinations, and observer orientations that we used to generate the pulse profiles shown in Figure 2. We have plotted only phased-averaged spectra here, although the calculation can derive spectra for arbitrary phase intervals. We have also plotted the corresponding EGRET data for the Crab pulsar (Nolan et al. 1993). Note that we have chosen the flux normalization in each plot to match the Crab data (eye fits only).

The spectra in Figures 4*a*–4*c*, all of which correspond to doubly peaked pulse profiles, are generally consistent with the observations from 50 MeV to at least 1 GeV, where both the data and the model values show a quasi-power-law behavior. The figures show variations in the model spectra at energies over ~1 GeV, where in general they begin to drop off rapidly due to the increasing efficiency of magnetic pair conversion at these energies. Such turnovers are a well known characteristic of polar cap cascades (e.g., Daugherty & Harding 1982). The energies at which they occur and their steepness are both sensitive to the primary electron distribution as well as other cascade parameters such as the surface magnetic field. In particular, the turnovers are expected to occur at higher energies for uniform primary beams, since electrons on field lines interior to the polar cap produce significant numbers of CR photons that travel almost parallel to the magnetic axis and hence escape pair conversion in the magnetic field.

Our results suggest that at least for our standard parameters, the uniform primary electron distribution (Fig. 4*a*) is better able to account for the full range of EGRET observations than the pure rim distribution of Figures 4*b* and 4*c*. The rim models tend to turn over at lower energies than the observations indicate. We can obtain better fits by assuming a lower magnetic field, although our standard value of 1 TG is already below the ~4 TG usually assumed for the Crab pulsar. This finding is in contrast to our results for the pulse profiles, which suggest that the rim models produce pulse widths closer to the observed values than uniform-beam models. Future calculations should determine whether an intermediate primary distribution, with at least some concentration near the rim, might improve the fits to both the spectral and profile data.

We should note that these spectra reflect only three physical processes, namely CR, $1 - \gamma$ pair production, and (quantized) SR. It may be significant that our model spectra appear to be generally consistent with the EGRET Crab observations from

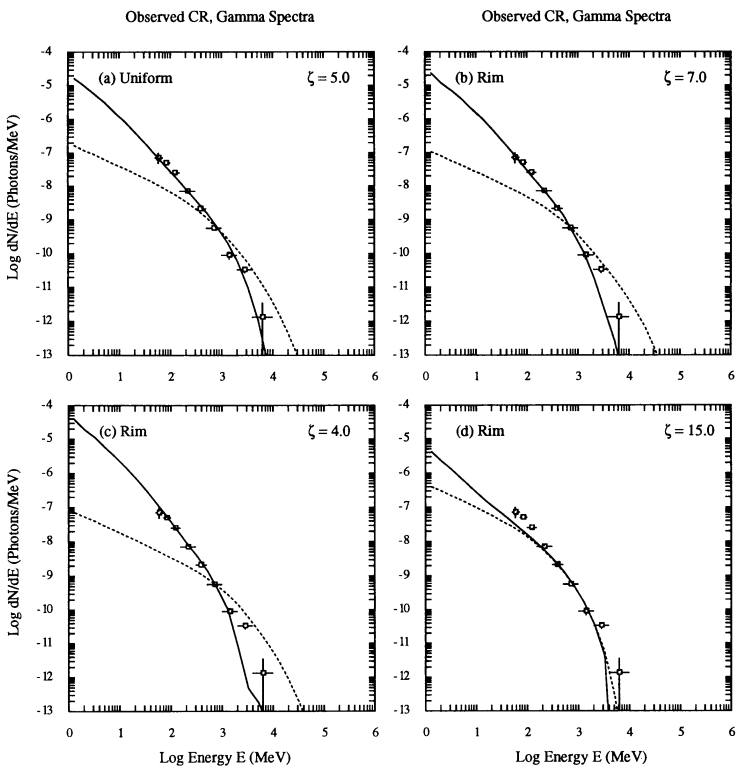

FIG. 4.—Model photon spectra, as seen from same observer directions used for pulse profiles in Fig. 2. All spectra are averaged over full period and normalized to match EGRET data points (also shown), using eye fits only. Solid lines correspond to escaping cascade photons, while dashed lines show pure CR spectra emitted by primary electrons (neglecting cascade effects). (*a*) Uniform primary beam, for $\zeta = 5°$. (*b*) Rim beam, $\zeta = 7°$. (*c*) Rim beam, $\zeta = 4°$. (*d*) Rim beam, $\zeta = 15°$ (corresponds to singly peaked profile in Fig. 2*d*).

50 MeV to at least ~1 GeV, even though our present simulation does not include Comptonization by either primary or secondary electrons. However, in order to obtain reliable spectra below the EGRET energy range we anticipate that Comptonization effects must be taken into account.

Our model results are also in similar general agreement with the spectra observed from the other sources described in § 1, although we should cite two notable exceptions. Both the second peak of the Geminga profile (Mayer-Hasselwander et al. 1994) and the phase-averaged emission from PSR 1055−52 (Fierro et al. 1993) show spectra even harder than the pure CR emission spectra in our model. However, it may still be possible to account for these spectra by including Comptonization, or by assuming that the radiating primaries are accelerated over extended distances above the polar caps.

6. DISCUSSION

The model of nearly aligned rotators proposed by Sturner & Dermer (1994) differs from ours in two essential ways. First, they assume that the primary acceleration energies are one to two orders of magnitude lower ($\gamma \sim 10^5$–10^6). Such values are too low for CR-initiated cascades to reproduce the observed spectra. They also argue that the primaries lose their energies by Comptonizing collisions with ambient optical, UV, and soft X-ray photons. The hard gamma spectrum of Comptonized photons thus replaces CR photons as the initiators of pair cascades. By making suitable assumptions about the soft photon intensities, they produce model pulse profiles and spectra in reasonable agreement with observations. In particular, for the Crab they assume that the soft photon background is beamed, rather than emitted isotropically from the stellar surface. They justify this assumption by noting that the soft pulsed emission from the Crab is in phase with the gamma emission (although the Crab is the only known gamma-ray pulsar for which this is the case). In other pulsars, which may not have a strongly beamed soft-photon source intersecting the path of the primary electrons, the resultant rate of Comptonization may be too low to account for the observed gamma emission.

The Sturner & Dermer (1994) model is similar to our CR-initiated cascade model with respect to estimated beaming factors (see § 4). For nearly aligned rotators, the narrow beams predicted by equation (1) help both models to account for the observed gamma-ray flux based on the predicted primary electron luminosity (Goldreich & Julian 1969). For a uniform primary distribution over the polar cap, the instantaneous gamma-ray flux due to a given luminosity is enhanced by the factor $2/(1 - \cos \theta_b)$ over the value for isotropic emission. In the context of their model, Dermer & Sturner (1994) have used this beaming factor to estimate the number of detectable gamma-ray pulsars, which they find to be compatible with the observations. We should note that the beaming factors may be even more favorable if the accelerated primaries are concentrated around the rim of the polar cap.

However, these small beam widths also imply that the chance of observing any given pulsar from the Earth is $\sim 10^{-2}$. As we demonstrated in § 4, the probability of observing well-separated double pulses from any of these objects is even smaller. In spite of the poor statistics, it seems hard to reconcile such estimates with either the fraction of gamma-ray pulsars

observed among the known supernova remnants, or the fraction which have a double-pulse structure. The "observability" criterion may in fact be a serious difficulty for nearly aligned rotator models, unless the polar caps are at least somewhat larger than the traditional estimate equation (1). On the other hand, we note that larger polar caps are actually to be expected if plasma and inertial effects are properly taken into account (e.g., Michel 1991). Increases by a factor ~ 2–3 should still be compatible with the luminosity constraints mentioned above, especially for hollow cone emission. Since the nearly aligned rotator model can otherwise account for so many spectral and temporal features of the gamma emission, we feel that the question of polar cap size requires closer scrutiny.

We have made preliminary simulations of CR-induced cascades using larger polar cap radii. Our results to date indicate that the most immediate effect of increasing θ_{pc} is to move the electrons to field lines with greater curvature, which enhances both the intensity and peak energy of the CR emission. This in turn extends the subsequent pair cascade to higher generations, producing generally softer gamma spectra if the "standard" parameters of Table 1 are used. We have been able to obtain spectra consistent with observations by using combinations of lower initial primary electron energies and surface B-fields.

Observations at other wavelengths may provide evidence for or against nearly aligned rotator models. One serious problem arises in the case of the Crab, where both of the optical pulses exhibit wide polarization swings in the same sense. Since this emission is in phase with the gamma peaks, it would seem plausible that it is produced in the same region of the magnetosphere. However, it is still unclear whether the optical polarization swings are directly related to the rotation of magnetic field lines. Since the radio emission is also in phase and does not exhibit similar polarization swings, the evidence is inconclusive.

TABLE 1

STANDARD MODEL PARAMETERS

Parameter	Value
Neutron star radius	$a = 10^6$ cm
Surface magnetic field	$B = 10^{12}$ G
Maximum primary electron energy	$E_p = 10$ TeV
Primary injection height above surface	$h = 0$ cm

The simple polar cap geometry considered in our model also suggests that the pulsating thermal X-ray emission expected from polar cap heating (or cooling) might show a single broad peak at a phase about midway between the two gamma peaks corresponding to rim emission. Recent observations of pulsed X-ray emission from Vela (Ögelman et al. 1993), Geminga (Becker et al. 1993; Halpern & Ruderman 1993), and PSR 1055−52 (Ögelman & Finley 1993) indicate that the X-ray emission profile is more complicated than this simple model would predict, but there is some suggestion that in the case of Geminga a thermal component may lie between the two gamma peaks.

Finally, we should note that neither our model nor that of Sturner & Dermer (1994) is incompatible with the possibility of gamma emission elsewhere in the magnetosphere, in particular from outer gaps (Cheng, Ho, & Ruderman 1986a, b).

The authors gratefully acknowledge support for this work from NASA grant NAG 5-2023.

REFERENCES

Arons, J. 1983, ApJ, 266, 215
Baring, M. G. 1988, MNRAS, 235, 51
Becker, W., et al. 1993, A&A, in press
Bennett, K., et al. 1977, A&A, 56, 469
Bertsch, D. L., et al. 1992, Nature, 357, 306
Cheng, K. S., Ho, C., & Ruderman, M. A. 1986a, ApJ, 300, 500
———. 1986b, ApJ, 300, 522
Daugherty, J. K., & Harding, A. K. 1982, ApJ, 252, 337
———. 1983, ApJ, 273, 761
Dermer, C. D., & Sturmer, S. J. 1994, ApJ, 420, L75
Erber, T. 1966, Rev. Mod. Phys., 38, 626
Fierro, J. M., et al. 1993, ApJ, 413, L27
Goldreich, P., & Julian, W. H. 1969, ApJ, 157, 869
Halpern, J. P., & Holt, S. S. 1992, Nature, 357, 222
Halpern, J. P., & Ruderman, M. 1993, ApJ, 415, 286
Harding, A. K. 1981, ApJ, 245, 267
Harding, A. K., & Daugherty, J. K. 1992, in Isolated Pulsars, ed. K. A. Van Riper & C. Ho (Cambridge: Cambridge Univ. Press), 279
Harding, A. K., & Preece, R. D. 1987, ApJ, 319, 939
Hermsen, W., et al. 1992, in AIP Conf. Proc. 280, Compton Gamma Ray Observatory (New York: AIP), 204
Kanbach, G. 1990, in EGRET Science Symposium (NASA CP-3071), 101
Kanbach, G., et al. 1994, in preparation
Kniffen, D. A., et al. 1975, Proc. 14th Internat. Cosmic-Ray Conf. (Munich), 1, 100
Mayer-Hasselwander, H. A., et al. 1994, ApJ, 421, 276
Michel, F. C. 1982, Rev. Mod. Phys. 54, 1
———. 1991, Theory of Neutron Star Magnetospheres (Chicago: Univ. Chicago Press)
Nolan, P. L., et al. 1993, ApJ, 409, 697
Ögelman, H., & Finley, J. P. 1993, ApJ, submitted
Ögelman, H., et al. 1993, Nature, 361, 136
Ruderman, M. A., & Sutherland, P. G. 1975, ApJ, 196, 51
Sturner, S. J., & Dermer, C. D. 1994, ApJ, 420, L79
Sturrock, P. A. 1971, ApJ, 164, 529
Thompson, D. J., et al. 1992, Nature, 359, 615
Wilson, R. B., et al. 1992, IAU Circ. 5429